PROCEEDINGS OF SCIENCE

Classical simulation of quantum $\lambda\phi^4$

Tzahi Yavin*
Department of Physics and Astronomy, York University
Toronto, ON Canada M3J 1P3
E-mail: t_yavin@yorku.ca

Takayuki Hirayama
USTC Shanghai Institute for Advanced Studies, 99 Xiupu Road
Pudong, Shanghai, China 201315
E-mail: hirayama@ustc-sias.cn

Bob Holdom
Department of Physics, University of Toronto
Toronto, ON Canada M5S 1A7
E-mail: bob.holdom@utoronto.ca

Roman Koniuk
Department of Physics and Astronomy, York University
Toronto, ON Canada M3J 1P3
E-mail: koniuk@yorku.ca

We consider the classical time evolution of a real scalar field in two dimensional Minkowski space with a $\lambda\phi^4$ interaction. All the modes are initialized with an amplitude that gives the zero-point energy spectrum of the corresponding quantum field theory, and the trajectories are averaged over the random phase of each mode. By comparing the masses extracted from correlation functions to the one- and two-loop quantum contributions to mass renormalization, we find that the classical evolution incorporates loop effects of the quantum theory. We also compare to Monte Carlo simulations of the quantum theory and find that the classical scheme uses a tiny fraction of the CPU time.

XXIIIrd International Symposium on Lattice Field Theory
25-30 July 2005
Trinity College, Dublin, Ireland

*Speaker.

PoS(LAT2005)254

1. Introduction

In quantum field theory, the vacuum is filled with zero-point energy to which each mode contributes $\hbar\omega/2$. This picture raises the question, what dynamics would emerge in an interacting classical field theory if each mode is initialized with energy $\hbar\omega/2$. If we assume the phase of each mode is randomly distributed, then Lorentz invariant correlation functions arise upon averaging over phases. Classical zero-point fluctuations of *free massless* scalar and vector fields, the Lorentz invariance thereof, and the effects of phase averaging, have been considered before, most notably by Boyer [1].

In [2], two of the present authors found critical and strong coupling behavior in classical $\lambda\phi^4$ theory that is strikingly similar to what is known about the quantum field theory. They also developed a perturbative expansion of the classical theory in the continuum and found a loop expansion very similar, but apparently not identical, to that of quantum field theory. Here we attempt a more quantitative comparison of the classical and quantum theories, where both are defined on the lattice. Our interest is not in the continuum limit of these lattice theories, or their critical behavior; we wish to compare physical masses that are safely above the inverse size of the systems, and safely below the inverse lattice spacing. We focus on the loop corrections to these masses.

2. Time Evolution

We study a classical $\lambda\phi^4$ theory in 1+1 dimensional Minkowski space on a lattice with an action

$$S = \sum_i \sum_{j=0}^{N-1} \frac{\dot{\phi}^2(i,j)}{2} - \frac{(\phi(i,j+1)-\phi(i,j))^2}{2} - \frac{m_0^2}{2}\phi^2(i,j) - \frac{\lambda}{4}\phi^4(i,j), \tag{2.1}$$

where $\hbar = c = a = 1$, and a is the lattice spacing along the x direction. The integers i and j label the sites in the t and x directions, and j runs from 0 to $N-1$. A periodic boundary condition is imposed along the x direction, i.e. $\phi(i,N) = \phi(i,0)$. The equations of motion are obtained from the action and we adopt the leapfrog method, which is reversible and has second order accuracy, to numerically integrate them.

To realize the $\hbar\omega/2$ contribution of each mode to the zero-point energy, the initial configuration of interest to us is

$$\phi_0(i,j) = \sum_{k=-N/2}^{N/2-1} \frac{1}{\sqrt{N\omega_k}} \cos(\omega_k a_t i + \frac{2\pi k}{N} j + \theta_k), \tag{2.2}$$

where $\omega_k^2 = 4\sin^2(\pi k/N) + \mu^2$ is the lattice dispersion relation, a_t is the lattice spacing along the time direction, and θ_k is a phase uniformly distributed over $[0, 2\pi)$. We leave the mass μ as a parameter over which we iterate, since the physical mass will be different from the bare mass m_0.

The key point is that we use (2.2) to specify the initial conditions, $\phi(0,j) = \phi_0(0,j)$ and $\dot{\phi}(1/2,j) = \dot{\phi}_0(1/2,j)$, but evolve forward in time with $\lambda \neq 0$ to investigate the dynamics of the interacting theory. We obtain expectation values by repeatedly starting from different sets of random

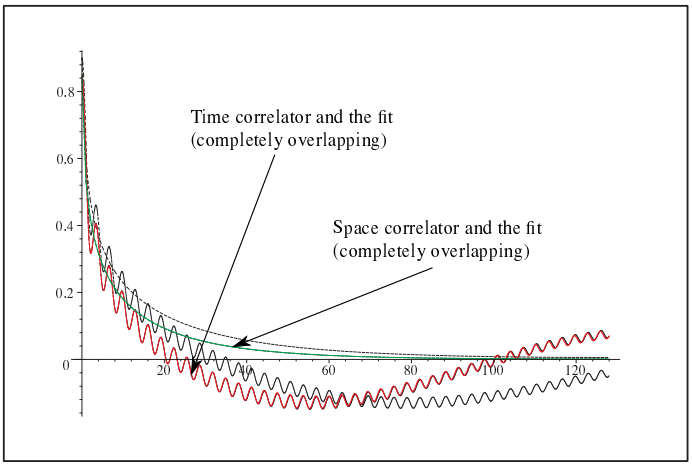

Figure 1: Time (wavy) and space (smooth) correlators for $N = 256$, $m_0^2 = 51/N^2$, $\lambda = 20/N^2$, and $t_f = 3N/4$; for comparison we also display the significantly different free correlators (black curves) with $\mu = m_0$, to show the effect of the mass renormalization.

phases. We use $\langle\cdot\rangle$ to denote this averaging, which gives an interesting indication of the emergence of quantum effects if we compute the expectation values

$$\langle\phi_0(i,j)\phi_0(i',j')\rangle = \sum_{k=-N/2}^{N/2-1} \frac{1}{2N\omega_k}\cos(\omega_k a_t(i-i') + \frac{2\pi k}{N}(j-j')) \tag{2.3}$$

$$= \mathrm{Re}\langle 0|T\phi(i,j)\phi(i',j')|0\rangle. \tag{2.4}$$

The r.h.s of the second line is just the real part of the Feynman propagator, and thus implies that the mass shift induced from the classical interaction term is exactly the same as the one-loop mass correction in quantum field theory.

We calculate time, space, and zero-mode time correlators with respect to the final time slice $t_f = a_t i_f$, which are defined respectively as:

$$G_t(i) \equiv \left\langle \frac{1}{N}\sum_{j=0}^{N-1}\phi(i_f,j)\phi(i_f-i,j)\right\rangle, \qquad G_x(j) \equiv \left\langle \frac{1}{N}\sum_{j'=0}^{N-1}\phi(i_f,j)\phi(i_f,j+j')\right\rangle,$$

$$G_0(i) \equiv \left\langle \frac{1}{N^2}\sum_{j,j'=0}^{N-1}\phi(i_f,j)\phi(i_f-i,j')\right\rangle.$$

Any of these can be used to extract mass, and we find that G_x is the least reliable, and that G_0 and G_t tend to agree well with each other. We concentrate on the time correlator G_t.

Fig. 1 demonstrates some important features of the classical simulation: (i) the system evolves towards the renormalized physical mass from the initial condition; (ii) the masses from the various correlators agree. This is an indication that Lorentz symmetry breaking due to lattice effects is not significant, and (iii) the physical mass can be determined to high accuracy. To within a percent or two all of the mass shift is due to the one-loop renormalization.

3. A Precision Measurement of Mass

The one-loop graph on a lattice with discrete space and continuous time is given by

$$\Pi(m) = \frac{1}{N}\sum_k \int \frac{dk'}{2\pi} \frac{1}{k'^2 + 4\sin^2(\pi k/N) + m^2} = \frac{1}{2N}\sum_k \frac{1}{\sqrt{4\sin^2(\pi k/N) + m^2}}. \tag{3.1}$$

This mass renormalization effect can be used to define the one-loop gap equation,

$$m^2_{\rm gap} = m_0^2 + 3\lambda\Pi(m_{\rm gap}). \tag{3.2}$$

Self-consistent solutions $m_{\rm gap}$ of this equation effectively sum up graphs with chains of bubbles, where each bubble represents Π, and allow the definition of a dimensionless coupling $g \equiv \lambda/m^2_{\rm gap}$. The one-loop graph is the only (log) divergent graph in this theory, and so the gap equation provides a useful representation of the physics for quite a large region of the m_0^2-λ plane.

For the example in Fig. 1 we have $g = 0.2$ and $m^2_{\rm gap} = 101.7/N^2$, to be compared with the mass extracted from the simulation of $m^2 = 100/N^2$. Given that there are two-loop corrections to the gap mass that are not included in the one-loop gap equation, our goal then is to decide whether the difference between our extracted mass and the gap mass is consistent with the size of the two-loop corrections from quantum field theory. At least at weak coupling we have seen that the evolving classical field quickly settles down to a stable configuration. Our prescription is to average over twenty equally spaced values of t_f up to a final time $t_f = 10N$ (a temporal extent 10 times the spatial extent) to obtain a mass. We then average between $10N$ and $20N$ to obtain a second mass. If the second mass does not deviate significantly from the first, then we accept the first mass as a reliable extracted mass.

4. Comparison to Quantum Methods

In the lattice quantum field theory we impose a periodic boundary condition along the time direction as well, and take $a_t = a = 1$ rather than $10a_t = a = 1$ in the classical simulation. The action is

$$S = \sum_{i,j=0}^{N-1} \frac{(\phi(i+1,j)-\phi(i,j))^2}{2} + \frac{(\phi(i,j+1)-\phi(i,j))^2}{2} + \frac{m_0^2}{2}\phi^2(i,j) + \frac{\lambda}{4}\phi^4(i,j). \tag{4.1}$$

With this different lattice regularization the one-loop self-energy graph and gap equation now become

$$\Pi_{\rm E}(m) = \frac{1}{N^2}\sum_{k,k'=-N/2}^{N/2-1} \frac{1}{4\sin^2(\pi k/N) + 4\sin^2(\pi k'/N) + m^2}, \tag{4.2}$$

$$m^2_{\rm Egap} = m_0^2 + 3\lambda\Pi_{\rm E}(m_{\rm Egap}), \tag{4.3}$$

with the subscript E standing for Euclidean. The resulting values $m_{\rm Egap}$ and $g_{\rm E}$ will thus differ from $m_{\rm gap}$ and g from our previous gap equation, and the behavior in the m_0^2-λ plane of these two theories will be different. The reason for the difference is that $\Pi_{\rm E}(m) \to 1/m^2$ as $m \to 0$ while $\Pi(m) \to 1/m$. Previous Monte Carlo simulations of the quantum theory [3] put the value of the critical coupling at $g = 10.24$ [1], and that is where the physical mass is expected to vanish.

[1] The critical coupling obtained from density matrix renormalization group methods [4] is 9.98.

In our quantum simulations we start with a hot start, and our updating scheme is the heat-bath algorithm followed by a Wolff step to reduce critical slowing down [5]. We monitor physical quantities such as the size of the Wolff clusters, the action, and the autocorrelation time of various operators. The physical mass is obtained by fitting the correlation function $G_E(i) \equiv \left\langle \frac{1}{N^3}\sum_{i',j',k'=0}^{N-1}\phi(i',j')\phi(i+i',k')\right\rangle$ to a cosh or a decaying exponential. We find that it gives physical masses compatible with the gap equation and that the mass extracted at strong coupling is also consistent with the expected critical behavior. The decrease of the physical mass towards zero as $g_{\rm E}$ is increased serves as one method for the determination of the location of the critical line. For another, the order parameter $\Phi = \frac{1}{N^2}\sum_{i,j=0}^{N-1}\phi(i,j)$ and its histogram can be studied as the size of the lattice is changed (see [3]).

5. The Two-Loop Effect

At leading perturbative order the difference between the physical mass and the gap mass is determined by a single two-loop diagram, the "sunset" diagram, which is given by

$$\Pi_{2\rm E}(m,k) \;=\; \frac{1}{N^4}\sum_{\{p_1,p_2,q_1,q_2\}=-N/2}^{N/2-1} G(p_1+k,p_2)G(q_1,q_2)G(p_1+q_1,p_2+q_2), \qquad (5.1)$$

where $G^{-1}(p_1,p_2) = 4\sin^2(\pi p_1/N) + 4\sin^2(\pi p_2/N) + m^2$ and k represents external momentum. This calculation gives a correction to the 2-point function at what corresponds to space-like external momentum, since this is a Euclidean quantum theory, and we find that $\Pi_{2\rm E}(m,k)$ monotonically increases as $k \to 0$. The classical theory however has Lorentzian signature, and so we actually need Π_2 at the time-like on-shell momentum. We will use $\Pi_{2\rm E}(m,0)$ as an estimate for this. Our quantum simulation data supports $\Pi_{2\rm E}(m,0)$ as a good estimate of the difference between the physical and gap masses for couplings as large as $g \approx 0.6$. As a further check we have directly estimated the single three-loop graph using the same technique as above (for smaller lattices) and found that it is $\lesssim g/2$ times the size of the two-loop graph.

We therefore consider a g^2 improved two-loop gap equation of the form

$$m^2_{\rm gap} = m_0^2 + [1-\varepsilon(m_{\rm gap})]3\Pi(m_{\rm gap})\lambda - 6\Pi_{2\rm E}(m_{\rm gap},0)\lambda^2. \qquad (5.2)$$

We have inserted a correction factor in the λ term to account for possible lattice artifacts - it is important to account for this because a small correction in the λ term can compete in size with the λ^2 term. This gap equation can be considered as a quantum model to be tested against the classical simulation data. Our strategy then is to use (5.2) as a one parameter model for the extracted physical mass $m_{\rm phys}$ from the classical simulation. We run the simulation for a range of values of m_0 and λ that produce values for $m_{\rm phys}$ very close to a fixed $m_{\rm gap}$, and thereby determine $\varepsilon(m_{\rm gap})$ through a best fit. We use 5000 trajectories for each determination of a mass. For the four values $m^2_{\rm gap} = (60,80,100,140)/N^2$ we find $\varepsilon(m_{\rm gap}) \approx (0.032, 0.029, 0.029, 0.029)$.

To test the quantum model for $m_{\rm phys}$ we isolate the g^2 dependence to get

$$g^2 = -\{m^2_{\rm phys} - m_0^2 - [1-\varepsilon(m_{\rm gap})]3\Pi(m_{\rm gap})m^2_{\rm gap}g\}/6\Pi_{2\rm E}(m_{\rm gap},0)m^4_{\rm gap}. \qquad (5.3)$$

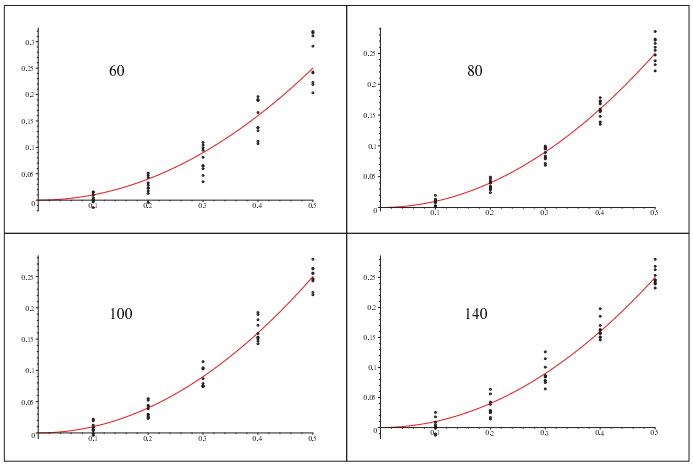

Figure 2: Plots showing the g dependence of the r.h.s of (5.3) using the classical simulation. The graphs are labelled by m^2N^2 and the red solid line is the g^2 quantum field theory prediction. Each plot displays the results of 10 different random number seeds, which give an indication of the errors.

We then determine the r.h.s from the classical simulation for a fixed $m_{\rm gap}$ and for a range of m_0 and g that give $m_{\rm phys} \approx m_{\rm gap}$. This is displayed in the plots of Fig. 2 where we see the residual quadratic dependence on g, and compare to the superimposed g^2 line of the quantum model. (The points would lie along a straight line if there was no g^2 effect.). These plots show that the results of the classical simulation are very well described by the quantum model, where the coefficient of the λ^2 term is given by the sunset diagram of quantum field theory. This is our main result.

References

[1] T. H. Boyer, *Random electrodynamics: The theory of classical electrodynamics with classical electromagnetic zero-point radiation, Phys. Rev.* **D11** (1975) 790-808; *General connection between random electrodynamics and quantum electrodynamics for free electromagnetic fields and for dipole oscillator systems, Phys. Rev.* **D11** (1975) 809-830; *Conformal symmetry of classical electromagnetic zero-point radiation, Found. of Phys.*, Vol. 19, No. 4 (1989) 349-365.

[2] T. Hirayama and B. Holdom, *Classical Simulation of Quantum Fields I*, `hep-th/0507126`.

[3] W. Loinaz and R. S. Willey, *Monte Carlo calculation of critical coupling constant for continuum ϕ_2^4, Phys. Rev.* **D58** (1998) 076003 [`hep-lat/9712008`].

[4] T. Sugihara, *Density matrix renormalization group in a two-dimensional $\lambda\phi^4$ Hamiltonian lattice model, JHEP* **0405** (2004) 007 [`hep-lat/0403008`].

[5] U. Wolff, *Collective Monte Carlo updating for spin systems, Phys. Rev. Lett.* **62** (1989) 361-364; R. C. Brower and P. Tamayo, *Embedded dynamics for ϕ^4 theory, Phys. Rev. Lett.* **62** (1989) 1087-1090.